Spatial Neglect Detection and Field of View Estimation Using a Novel Brain-Computer Interface

by

Deniz Kocanaogullari

BS in Electronics and Communication Engineering, Istanbul Techincal University, 2019

Submitted to the Graduate Faculty of

the Swanson School of Engineering in partial fulfillment

of the requirements for the degree of

Master of Science

University of Pittsburgh

2021

UNIVERSITY OF PITTSBURGH

SWANSON SCHOOL OF ENGINEERING

This thesis was presented

by

Deniz Kocanaogullari

It was defended on

April 2, 2021

and approved by

Ervin Sejdic, PhD, Associate Professor, Department of Electrical and Computer Engineering

Zhi-Hong Mao, PhD, Professor, Department of Electrical and Computer Engineering

Thesis Advisor: Murat Akcakaya, PhD, Associate Professor, Department of Electrical and Computer Engineering

Spatial Neglect Detection and Field of View Estimation Using a Novel Brain-Computer Interface

Deniz Kocanaogullari, M.S.

University of Pittsburgh, 2021

Spatial neglect (SN) is a neurological syndrome in stroke patients, commonly due to unilateral brain injury. It results in inattention to stimuli in the contralesional visual field. The current gold standard for SN assessment is the behavioral inattention test (BIT). BIT includes a series of pen-and-paper tests. These tests can be unreliable due to high variability in subtest performances; they are limited in their ability to measure the extent of neglect, and they do not assess the patients in a realistic and dynamic environment. In this thesis, we present an electroencephalography (EEG)-based brain-computer interface (BCI) that utilizes the Starry Night Test to overcome the limitations of the traditional SN assessment tests. Our first goal with the implementation of this EEG-based Starry Night neglect detection system is to provide a more detailed assessment of SN. Specifically, to detect the presence of SN and its severity. To achieve this goal, as an initial step, we utilize a convolutional neural network (CNN) based model to analyze EEG data and accordingly propose a neglect detection method to distinguish between stroke patients without neglect and stroke patients with neglect. In this project, we also propose an EEG-based BCI that utilizes an augmented reality (AR) headset to present the Starry Night Test to overcome the limitations of the BIT. The ultimate goal of this implementation is to provide a more nuanced assessment of SN on patients with stroke and also to overcome the limitations of computer screens by using an AR headset. As an initial step to achieve these goals, we use common spatial patterns (CSP) and create a classifier using linear discriminant analysis (LDA) to propose a field of view estimation method for stroke patients both with and without spatial neglect.

Table of Contents

List of Tables

List of Figures

Preface

First of all, I want to thank Dr. Akcakaya for all his support during these two years, both related to work and in life. Under his guidance, I was able to work with a productive team and improve myself as a researcher. I also want to thank Dr. Sarah Ostadabbas, Dr. George Wittenberg and all my labmates including my collaborators for all their supports during this study. I also thank my family whose support made a huge impact on my success my entire life. I would also like to thank Dr. Ervin Sejdic and Dr. Zhi-Hong Mao for accepting to be in my exam committee.

Lastly, I want to thank my brother, Dr. Aziz Kocanaogullari, who has supported me in every way since I was little and taught me everything I know. I was able to grow up to be a graduate student who conducts research thanks to him; hence, this thesis is dedicated to him.

1.0 Introduction

1.1 Spatial Neglect in Stroke Patients

Spatial neglect (SN) is a common disorder that arises after stroke and has been observed in 28.6% of stroke patients [9]. SN is a perceptual disorder characterized by inattention to stimuli in the contralesional visual field. People with SN usually display inattention to one side of themselves, such as inability to shave one side of the face or dress one side of their body. Lesions to the attentional networks [7], ventral frontal lobe, right inferior parietal lobe or superior temporal lobe can cause SN [14]. Left-side neglect is more common and often more severe compared to right-side neglect [34]. SN is a strong predictor of disability and it could possibly develop safety concerns; a diagnosis of SN is often accompanied by extended hospitalization [5], an increased risk of falling [11], and poor stroke recovery outcomes [10].

1.2 Assessment of Spatial Neglect

The current gold standard method is the Behavioral Inattention Test which consists of 6 subtests in the conventional test: line crossing, letter cancellation, star cancellation, figure and shape copying, line bisection, and representational drawing [52]. Majority of neglect assessment tests involve pen-and-paper tests[44]. It is difficult to determine SN using only one subtest and the drawing tests can be subjectively scored. Additionally, these tests to do not assess the patient in a realistic, dynamic environment; they are not sensitive to changes in neglect severity, and they are affected by compensatory strategies. Therefore, performance between subtests can also be highly variable [47]. Furthermore, BIT gives an overall score, which is compared to the established cutoff score to return a "yes-or-no" diagnosis of SN; it does not give the extent to which the patient has SN. These issues present a clinical need for an objective measurement of SN that will identify its presence as well as the severity.

There are also alternative methods for neglect assessment such as Catherine Bergego Scale. It is a performance-based assessment that evaluates the impact of neglect while completing daily activities [6]. Even though this assessment is shown to have stronger sensitivity than pen-and-paper tests, impact of compensatory strategies on the performance of the test is still unclear [6] and it is unclear whether the test has adequate sensitivity to change. Considering the limitations of the said pen-and-paper tests and performance-based assessments, it is clear that a more detailed and accurate assessment is needed.

1.3 Computer-based Spatial Neglect Assessment Methods

To overcome such limitations of pen-and-paper tests, computer-based spatial neglect assessment methods have been created. One category of such methods measure the reaction time of participants to certain targets that appear on a screen as reaction time is a quantitative measure that reflects attention during rehabilitation process [17]. One such example from the category is that a system was developed to project white squares on random locations on a computer screen along the horizontal meridian [4], and participants were asked to press a button when they observe the square and the corresponding response times were recorded. A more sophisticated version was created to emulate pen-and-paper tests that have distractors on the background [8]. In this version, a white circle has been added to the previous paradigm as a distractor. However, this test is static as both the target and distractor are non-moving. A dynamic driving simulator is designed to evaluate attention and to detect neglect [51]. In this paradigm, participants were asked to press a button when they detect a rectangle on the right, middle or left side of the screen while simultaneously following the traffic lanes.

fMRI has been utilized as an alternative to said methods for attention assesment [15]. One method using fMRI uses a box car fMRI design where participants were directed to focus on the center of the screen where a square is presented while distractors were shown on both sides of the screen [50]. In another project, a fixation cross is presented in the middle of the screen and participants were directed to focus on the cross. At the same time, a target

letter is presented either on the left or right side of the screen and participants were asked to observe that [31]. fMRI data evaluates the difference between attention and inattention cases and measures the oxygenation level in the brain, which has been proven to change in patients with acute stroke [25]. However, unlike electroencephalography (EEG), fMRI does not measure neural activation directly and it is more bulky and more expensive.

1.4 EEG-based Brain Computer Interfaces

EEG is used as the measurement modality because it is portable and more cost-effective than other brain imaging techniques. Moreover, it has very high temporal resolution. Furthermore, certain EEG features were shown to be associated with neglect: (i) on average there is an increase in N100 and P200 responses in the EEG of perceived targets compared to neglected targets in stroke patients and (ii) the N100a EEG component which is expected around 130-160ms after a stimulus, does not exist in the EEGs of neglect patients in response to contralesional stimuli. [18].

Due to said assets of EEG, it has been employed in several studies. Several EEG-based BCI's have been developed for motor imagery paradigms. In one example, participants were tasked to conduct a center-out cursor task, where the cursor was guided to one of the eight targets located on the computer screen [53]. Each dimension of the cursor movements is defined by a linear equation in which the independent variable is a weighted summation of mu and beta rhythm frequency bands that were associated with right- and left-hand imaginary movements. Another popular paradigm in EEG-based BCI systems is visual P300, which is an event-related potential component that is elicited in the process of decision making. One such example is typing systems, where a rapid serial visual presentation (RSVP) is presented on a computer screen. All letters in English alphabet and two symbols for backspace and space are presented in a three step presentation and EEG data is analyzed using regularized discriminant analysis for letter decision [3, 37]. In another example, circular Gabor gratings appear randomly in one of the four quadrants on the screen and participants were asked to observe them [19]. In this study, statistical differences were shown between

EEG corresponding to neglected and non-neglected targets; but, these differences were not used to creaste a test to identify acute stroke patients with neglect and the paradigm does not include any distractors which diversifies the test from real-life environment. In a different study, temporal and spatial attention were assessed by analyzing EEG [20]. Four auditory tasks were given to participants for analysis but similar to the previously mentioned study, this one also lacks a test design that is specifically built for identifying the presence of neglect.

EEG-based BCI's are also important for rehabilitation purposes. A project was developed for a tetraplagic patient whose residual activity of the upper limbs were restricted to their left biceps and to restore the hand grasp function. An electrical hand orthosis was created whose movements are dependent on EEG and the tetraplegic patient learned to operate the hand by mental imagination [43]. In another study, to control a functional electric stimulation system for overground walking an EEG-based BCI has been created for patients with paraplegia due to spinal cord [32]. A participant with spinal cord injury was recruited and underwent muscle reconditioning to facilitate standing and overground walking. Both BCI and functional electric stimulation system were integrated and participant was engaged in several real-time walking activities. Over the course of 19 weeks, participant was able to conduct operate the BCI-functional electric stimulation system successfully.

1.5 Contribution of the Study

In this study, we have utilized a modified Starry-Night Test to both collect data and create our own augmented reality based paradigm. Our novel BCI setup uses the Microsoft HoloLens goggle to visualize the paradigm, instead of a computer screen, to provide a better field-of-view coverage while also eliminating potential target misses and compensatory techniques from the participants that may create incorrect labeling or incorrect patterns in the EEG data. Participants in both methodologies were asked to complete a number of tasks for the conductors to collect time data for labeling and EEG data, with respect to 10-20 system, for analysis. Both of these tests are conducted by using the Starry-Night Test. From the time data, slow-response and fast-response labels were collected using a thresholding

method. By a feature extraction algorithm (common spatial patterns) and a linear classifier (linear discriminant analysis) we have analyzed the separability between slow-response and fast-response targets; both in an across-participants sense and participant-by-participant sense. Moreover, a deep neural network model (EEGNet) has been used to differentiate participants with and without spatial neglect by analyzing slow-response targets' filtered time-series EEG data, from both of the groups to detect the existence of spatial neglect in a participant with stroke. With the novel BCI setup and these analyses, we aim to provide healthcare providers with a setup that can be used to detect, and in the future rehabilitate, stroke patients with spatial neglect.

2.0 Methodology

Two different analyses have been conducted in this study: spatial neglect detection and slow response versus fast response analysis. For the first analysis, slow response data from patients with and without spatial neglect have been used to assess the existence of spatial neglect in stroke patients. The second analysis uses both slow response and fast response targets in order to detect potentially neglected targets universally among the entire participant population. As the second analysis is part of an ongoing research project, participant data that are used differ from each other and because of that participant information is separated between two analysis methods in this chapter.A flowchart representing the summary of this study can be seen in Fig. 1.

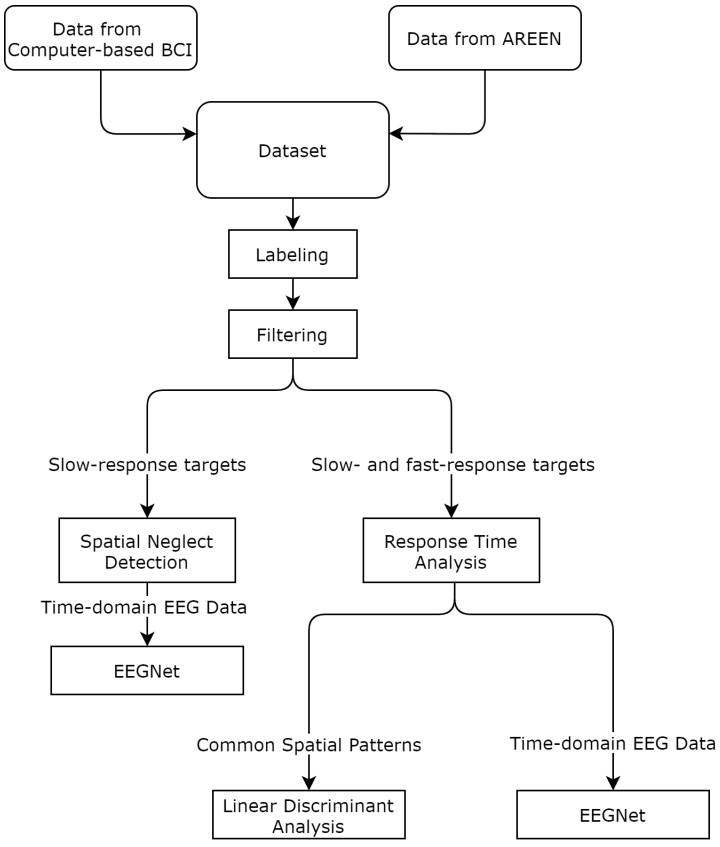

Figure 1: Flowchart summarizing the study

Following the flowchart, the study starts with data collection session from two different methodologies. Data collection has concluded for Computer-based BCI and data collection session for AREEN are ongoing. After combining the data that are available, entirety of the dataset is labeled using Otsu's thresolding [42] and filtered using an FIR filter. As we have conducted two different studies, then we select the corresponding data for each study. In the first study, EEG-based neglect detection, we have only used data collected with Computer-based BCI as data collection with AREEN started after that study began. In that study, we get slow-response targets from every participant, both with and without spatial neglect, and put the filtered time-series EEG data to a deep learning model called EEGNet [39]. The results we get from there provides the notion of neglect detection in stroke participants as it assesses the existence of spatial neglect. In the latter study, we get both slow-response and fast-response targets from 5 participants from Computer-based BCI framework and 5 participants from AREEN setup. Here, the study has two parts: across participants analysis for slow- versus fast-response targets and participant-wise analysis. In both of them, we get all 10 participants' data and put it through a feature extraction algorithm called common spatial patterns [35] to get features. After that, in slow- versus fast-response analysis, new features are classified using linear discriminant analysis [21] for assessing potentially neglected targets. EEGNet model used in the former study has also been used to show the shortcomings of deep learning models in our current dataset. In participant-wise analysis, the same modality has been used to create a generalizable model for rehabilitating participants with neglect.

2.1 Data Collection Techniques

2.1.1 EEG-based Starry Night Test

In this study, we used the modified version of previously designed EEG-based Starry Night Test [30]. The modification removed the spatial neglect stimulation to evaluate the existance of spatial neglect in stroke patients. Specifically, a participant's time-data and

EEG are recorded with respect to their visual stimuli corresponding on random locations where targets are shown to analyze both existence and severity of spatial neglect.

The participants are seated 114cm away from the screen, which corresponds to a viewing area of 17.23° by 9.74°. A modified version of the Starry Night Test [17] is used for the experiments. In this test, the screen is divided into an 8x8 grid and targets are shown in 64 random locations on this grid. A target appears 3 times in every location for a total of 192 targets. These targets are red dots which cover 0.22° of a person's visual field. They are shown for 66ms on the screen and the time between each target is randomized from 700ms to 2200ms. There are also distractors, which are smaller green dots that are shown randomly every 50-250ms. The reason for the randomized appearance of targets and distractors is to reduce the risk of seizure [22]. The paradigm can be seen in Fig 2.

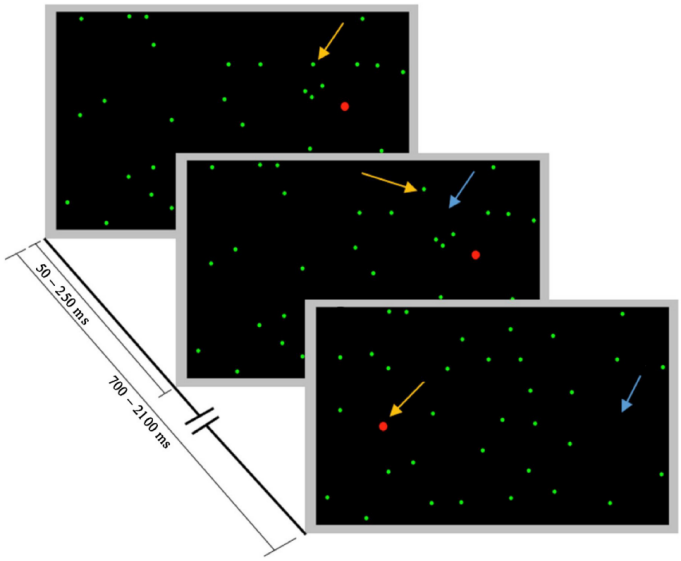

Figure 2: Starry Night Paradigm. This figure represents a single trial [30].

The experiment begins with a calibration session, where the targets stay on the screen until the participant presses a key on keyboard or for 3 seconds [17]. The response times corresponding to all targets are recorded. The number of targets and the occurences of both targets and distractors are the same with the EEG collection session. EEG is not collected during the calibration session in which we learn the ground truth for the neglected visual field. After collecting the time data for all of the 192 targets from 64 different locations, we

employ a thresholding method and get the median of each location's time data to employ majority voting for deciding on the label of each screen location.

EEG was collected through 16 electrodes located at Fp1, Fp2, F3, F4, Fz, Fc1, Fc2, Cz, P1, P2, C1, C2, Cp3, Cp4, P5 and P6 according to 10-20 system with sampling frequency of 256Hz.

2.1.2 AR-based EEG-guided Neglect Detection

AR-based EEG-guided Neglect detection, assessment, and rehabilitation, AREEN for short, is a research project aimed to develop an integrated multimodal tool for detection, assessment and rehabilitation of unilateral spatial neglect caused by stroke. Unlike standard BCI systems, using AR provides a more realistic daily living environment for participant and yields in better data quality. Microsoft HoloLens is a state-of-the-art AR device that is comprised of see-through holographic lenses with automatic pupillary distance calibration and provides 2.3 million total light points as holographic resolution. Wearing this AR headset holograms are able to be projected in front of the participants. Unlike previous BCI applications which provide fixed-location visual cues, our project provides a customized application which tracks participant's head position in real-time and projects the holographic visual cues dynamically in the participant's visual space.

The innovative AREEN system detects and maps visually neglected extra-personal space with high accuracy through continuous EEG-guided neglect detection. A snapshot of the AREEN system used by one of our participants is shown in Fig. 3.

2.1.2.1 Implementation Details

The application itself can be considered as a cascade of multiple applications in different platforms working as a whole. Unity has been used for HoloLens projection, where a modified version of Starry Night Test has been built specifically for AR. The test utilizes the see-through lenses where the targets and distractors are clearly seen without adding anything extra to participant's vision. The connection between a computer and Microsoft HoloLens system is completed via Bluetooth Low Energy (BLE) connection utilizing an Arduino kit.

AREEN system was developed in multiple platforms: the Starry Night Test for HoloLens is built on Unity, GUI for research conductor is built on MATLAB R2015a, EEG collection part is built on MATLAB R2015a by using gTec's MATLAB API and Bluetooth connection between HoloLens and PC is done by Arduino. The connection between hardware devices of AREEN can also be seen in Fig. 3.

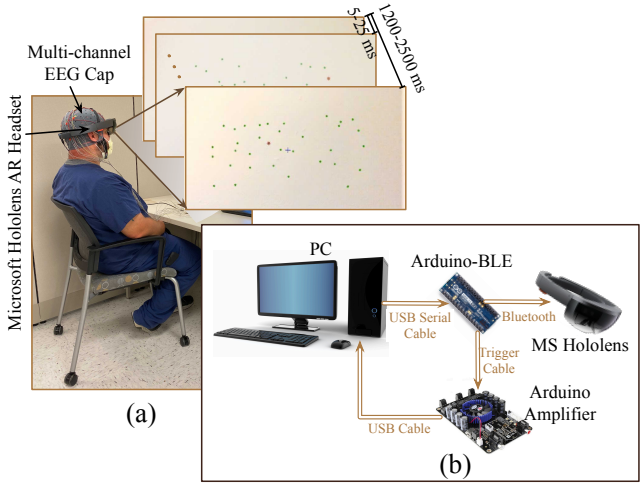

Figure 3: (a) Participant using AREEN system which presents the Starry Night Test paradigm. EEG electrodes are connected to the system for data collection. (b) Flowchart that represents connections within AREEN system.

The canvas is divided into 6×12 grids. The entirety of canvas is of size 0.564m · 0.288m and the depth is 1.14m. The duration between each red star, or a target, is randomly selected between 1.2s to 2.5s. The number of distractors, or green stars, that can be seen in Fig. 3, differ from 30 to 35 randomly and they stay on the canvas from 0.05s to 0.25s randomly. Targets are shown 216 times total, 3 times in each cell. They stay on the canvas for a maximum of 3s during the clicker-based assessment and FOV (field of view) test, and 0.066s in EEG-based assessment. Randomizing the appearance of targets and distractors reduces the risk of seizure [23]. The experimental modes and data collection process will be introduced in the next section.

2.1.2.2 Procedure of Data Collection

In order to achieve reliable detection and assessment of spatial neglect, AREEN system provides several modes. This part of AREEN system has been built using MATLAB. The modes are executed in the following order:

- Signal Check: This mode assures the stability of connection between computer and EEG amplifier and checks the quality of 16 channels' EEG signals in real time before experiments. Research conductors check EEG data visually in a real time sense.
- Field of View (FOV) Test: This mode allows the research conductor to calibrate field of view in HoloLens. It includes top (first two rows), left (2^{nd} and 3^{rd} columns), central (6^{th} and 7^{th} columns), and right (10^{th} and 11^{th} columns) FOV tests. In this session, only the red target is randomly presented in all cells of specific region three times every 1.2s to 2.5s. Each target object remained on the canvas for a maximum of 3s or until the participant pressed Clicker before the end of the 3s period. After session is over, HoloLens sends message to PC via BLE connection, and targets orders, neglect keys, and reaction times are saved and checked for adjusting headset position.
- Clicker-based Assessment: This mode is used to generate ground truth to label the EEG data by identifying the locations of the HoloLens canvas in which stimuli is neglected by the individuals with neglect, resulting in two class labels: neglected and not neglected canvas locations. Similarly, selecting "Clicker-base Assessment" in Modes menu on PC triggers this session to run independently following the same rules, but with green distractors presented every 0.05s to 0.25s and targets randomly appears in all 72 cells of the entire canvas three times. After session is over, HoloLens sends message to PC via BLE connection, and targets orders, neglect keys, and reaction times are saved for generating ground truth.
- EEG-based Assessment: During this mode, PC sends triggers to HoloLens for target presentation, meanwhile, the participant's EEG is recorded in response to visual stimuli shown on random locations on the HoloLens canvas to assess both existence and severity of neglect. After selecting this mode in Mode menu, PC activates the EEG amplifier to calibrate and configure parameters of collecting EEG data. Then the EEG amplifier

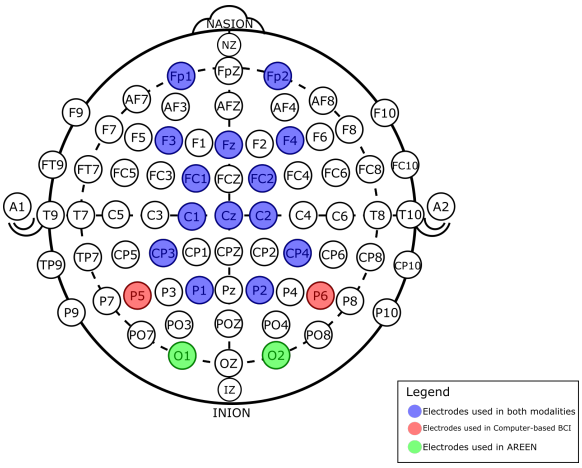

Figure 4: Image representing the International 10-20 system for EEG-MCN (EEG-Modified Combinatiorial Nomenclature). Electrodes that are used in both paradigms have been highlighted with blue, those that are only used in the first modality, Computer-based BCI, are highlighted with red and the electrodes that are only used in novel AREEN system are highlighted with green.

is informed by PC to start collecting EEG data and HoloLens is activated to display green distractors on canvas. After that, PC starts to send trigger to BLE module after a random period ranging from 1.2s to 2.5s measured from each trial onset. Once receiving a trigger, BLE module sends a 'message' to HoloLens via Bluetooth and amplifier over cable simultaneously to present a target on HoloLens canvas and mark the EEG signal. A target stays on the canvas for 0.066s and once it disappears, a new trial starts. The test continues until a total of 216 triggers are sent from PC which means that each of the 6×12 locations on the canvas were occupied by a target 3 times. After this session is done, HoloLens sends message to PC via BLE module, and triggers elapsed time of both HoloLens and PC, targets orders, neglect keys, and reaction times are saved for offline correcting trigger markers and EEG analysis.

EEG data, with AREEN system, are collected through 16 electrodes located at Fp1, Fp2, F3, F4, Fz, Fc1, Fc2, Cz, P1, P2, C1, C2, Cp3, Cp4, O1 and O2 according to 10-20 system with sampling frequency of 256Hz.

2.2 Preprocessing

In this study, we have used different data preprocessing methods for two different analyses. For labeling, we have used Otsu's thresholding [42] for separating slow- and fast-response targets.

2.2.1 Otsu's Thresholding

Otsu's method is a popular algorithm in signal processing. Basically, the algorithm returns a single intensity threshold that separates values into two classes. This threshold is determined by minimizing the intra-class variance, or equivalently, maximizing the inter-class variance.

The algortihm exhaustively searches for the specific value that minimizes the intra-class variance. This is defined as a weighted sum of variances of two classes:

$$\sigma_\omega^2(t) = \omega_0(t)\sigma_0^2(t) + \omega_1(t)\sigma_1^2(t) \tag{2.1}$$

where σ_i^2 are variance of the classes and ω_i are the weights; probabilities of the two classes separated by the threshold t. Then, the class probabilities $\omega_{0,1}(t)$ is computed from the L bins of the histogram:

$$\omega_0(t) = \sum_{t=0}^{t-1} p(i) \tag{2.2}$$

$$\omega_1(t) = \sum_{i=t}^{L-1} p(i) \tag{2.3}$$

As stated above, intra-class variance minimization is equivalent to inter-class maximization:

$$\sigma_b^2 = \sigma^2 - \sigma_w^2(t) = \omega_0(\mu_0 - \mu_T)^2 + \omega_1(\mu_1 - \mu_T)^2 \tag{2.4}$$

$$= \omega_0(t)\omega_1(t)[\mu_0(t) - \mu_1(t)]^2 \tag{2.5}$$

where the class means $\mu_0(t)$, $\mu_1(t)$ and μ_T are:

$$\mu_0(t) = \frac{\sum_{i=0}^{t-1} ip(i)}{\omega_0(t)} \tag{2.6}$$

$$\mu_1(t) = \frac{\sum_{i=t}^{L-1} ip(i)}{\omega_1(t)} \tag{2.7}$$

$$\mu_T = \sum_{i=0}^{L-1} ip(i) \tag{2.8}$$

and as $\omega_0\mu_0 + \omega_1\mu_1 = \mu_T$ and $\omega_0 + \omega_1 = 1$ this yields an effective thresholding algorithm.

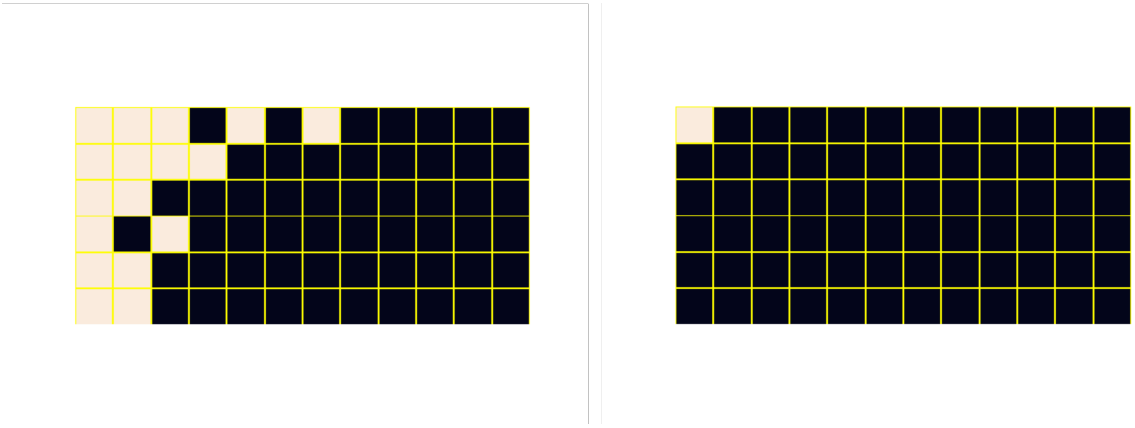

Figure 5: Field of view images of SN101 (left) and WSN102 (right). Note that as the participants were part of AREEN, the grid is 6x12. Black boxes represent that the target is potentially perceived and beige boxes represent targets that are potentially neglected. One can easily see that SN101 (left) missed one side of the grid nearly completely, due to the existence of spatial neglect.

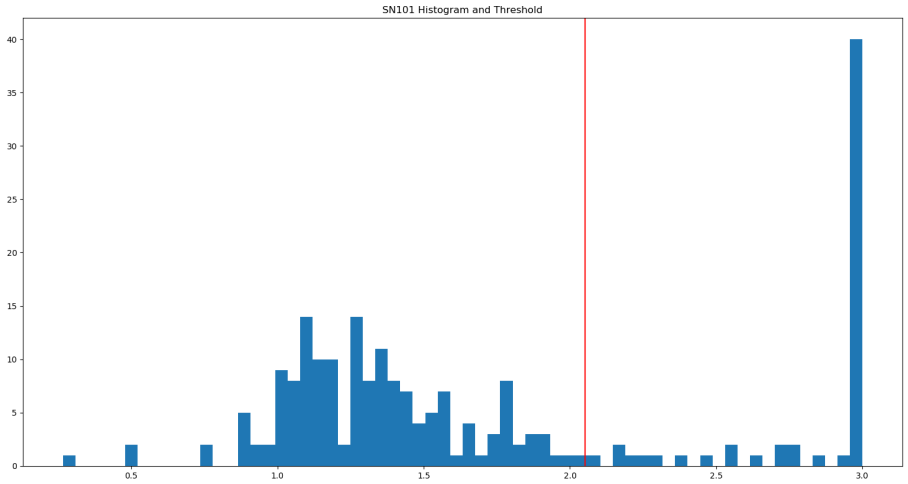

(a)

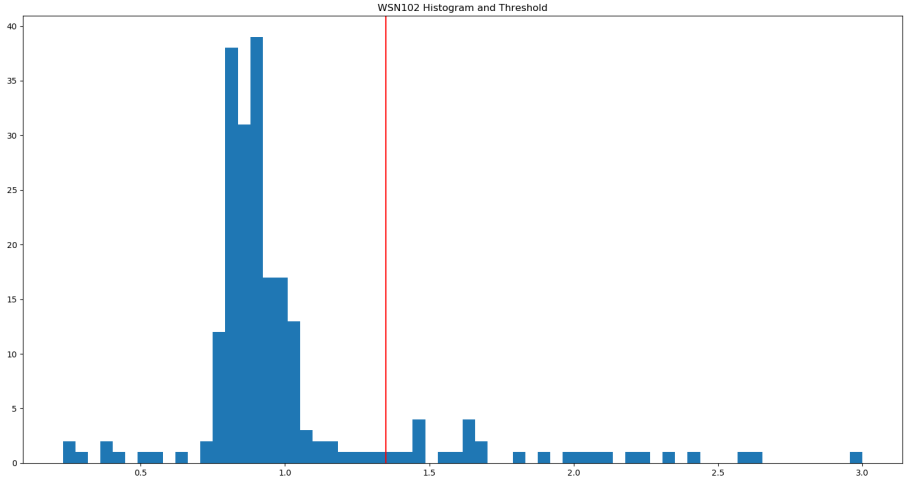

(b)

Figure 6: Histograms and threshold values found with Otsu's method. Note that these histograms come from the same participants as Fig 5.

2.2.2 Preprocessing in Spatial Neglect Detection

After the calibration session, the target locations corresponding to slow-time and fast-time response targets are identified. Specifically, to achieve this separation, a time threshold for every patient is calculated using Otsu's method [42]: if a target's corresponding response time is greater than the threshold value, it is considered as a 'slow-response target' or a neglected target; if it is smaller than the threshold value then it is a 'fast-response target' or an observed target. This procedure provides information about the perceived or potentially not perceived/neglected locations on the observed visual field of the computer screen and it is used as a ground-truth for the following EEG analysis. One such example where one session from two participants, one with spatial neglect and one without, can be seen in Fig. 5. Accordingly, EEG data are first processed through an 8^{th} order Butterworth band-pass filter with corner frequencies of 2 and 62 Hz, and then through a 4^{th} order notch filter with corner frequencies of 58 and 62 Hz, and EEG corresponding to slow-response and fast-response targets are separated from each other to be used in the following classification approach.

After filtering, as there is a minimum of 700ms between each target presentation during EEG collection based on the designed paradigm, see Fig. 2; 192 EEG segments, each 700ms long and time-locked to the presented targets, are extracted from each patient's recorded EEG data. As EEG is very person-specific, and we are aiming at a classification across individuals, first 500ms of the EEG segments are considered to include the desired response, and a baseline correction was applied to each segment using the last 200ms of their data. Baseline correction is achieved in the spectral domain such that the spectrum of the desired responses is corrected by the baseline spectrum of the baseline. These spectrum are computed through Fourier transforms with a Hamming window. After baseline correction, every channel is normalized using min-max normalization to generate a common scale for all data.

2.2.3 Preprocessing in Slow- versus Fast-response Analysis

After the clicker-based assessment, target locations corresponding to slow-response and fast-response targets are identified. In order to achieve this separation, Otsu's method [42] is used to create a time-threshold for every patient: if a target's corresponding response time is greater than the threshold, the target is considered as a slow-response target; if it is smaller than the threshold, then it is considered as a fast-response target. We follow a majority-voting procedure for 72 targets, which are shown three times on the test, before creating a threshold value. Specifically, we get the median value of all three showings of a target to get the time data corresponding to that specific target. Getting the median increases the number of slow-response targets in a way that is more robust compared to getting the mean in terms of outlier behaviour. This procedure provides information about potentially perceived or potentially neglected locations on the visual field and it is used as ground-truth to label EEG data. EEG data are first put through an 8^{th} order Butterworth filter with corner frequencies of 2Hz and 60Hz, and then through a 4^{th} order notch filter with corner frequencies of 58Hz and 62Hz.

After filtering, EEG data that are 700ms long and time-locked to the presented targets are extracted from each participant's recorded EEG data, for a total of 192 or 216 EEG segments, dependent of the dataset the data comes from. As EEG is very person-specific and we are aiming at a classification across individuals, an 200ms long EEG data before a target is presented is used for baseline correction. Baseline correction is done in the time domain such that the average value of the said 200ms part is calculated and the actual segment is corrected. After baseline correction, every channel is normalized using standard normalization, where the data is made zero-mean and unit variance, to create a common ground for the entirety of the data.

2.3 Classification Algorithms

2.3.1 Classification between Slow- versus Fast-response Targets for Field of View Estimation

A machine learning based classification algorithm is created to distinguish between slow-response and fast-response targets across stroke patients with and without neglect. More specifically, we apply linear discriminant analysis on top of common spatial patterns as a feature extraction algorithm [35]. Linear discriminant analysis is a generalization of Fisher's linear discriminant. As the last two channels differ in two different data collection methods, for across participants classification problem only the first fourteen channels of the reported channels were used, which are Fp1, Fp2, F3, F4, Fz, Fc1, Fc2, Cz, P1, P2, C1, C2, Cp3 and Cp4.

2.3.1.1 Linear Discriminant Analysis

Let $x_1, ..., x_N = \mathbf{X} \in \mathbb{R}^{Nxd}$ be a set of N samples belonging to C different classes. Linear Discriminant Analysis finds a linear projection $\mathbf{W} \in \mathbb{R}^{lxd}$ into a lower l-dimensional subspace L where $l = C - 1$. By this means, the linear combination of features $x_i\mathbf{W}^T$ are maximally separated in this space [24]. To find $\mathbf{W}$, one needs to solve the following optimization problem:

$$\arg\max_{\mathbf{A}} \frac{|\mathbf{A}S_b\mathbf{A}^T|}{|\mathbf{A}S_b\mathbf{A}^T|} \tag{2.9}$$

where S_b is the between-class scatter matrix and S_w is the within-class scatter matrix where their relationship to total scatter matrix is given by $S_b = S_t - S_w$. To find those matrices, we have to define the mean-centered observations of class c $\bar{\mathbf{X}}_c = \mathbf{X}_c - \mathbf{m}_c$ where $\mathbf{m}_c$ is the within-class mean vector. Thus, S_b and S_w become

$$\mathbf{S}_c = \frac{1}{N_c - 1}\bar{\mathbf{X}}_\mathbf{c}^T\bar{\mathbf{X}}_\mathbf{c} \tag{2.10}$$

$$\mathbf{S}_t = \frac{1}{N-1}\bar{\mathbf{X}}^T\bar{\mathbf{X}} \tag{2.11}$$

$$\mathbf{S}_w = \frac{1}{C}\sum_c \mathbf{S}_c \tag{2.12}$$

By solving the optimization problem given above one also maximizes the ratio of S_b and S_w. More specifically, this results in a set of projected observations of the same class resulting in low variance while a set of projected observations of the different class showing high variance in the resulting space L. To find the optimum solution for Eq. 2.9 one has to solve the general eigenvalue problem $S_b e = v S_w e$ where e is the set of eigenvectors associated with the projection matrix $\mathbf{W}$.

2.3.1.2 Common Spatial Patterns as Discriminative Features

Common spatial pattern (CSP) is an algorithm to calculate spatial filters and it is widely used in BCI systems. It was first proposed to classify imagined hand movements by using multi-channel EEG [45]. More specifically, the goal is to design a pair of spatial filters such that the filtered signal's variance is maximum for one class while minimal for the other, and vice versa. Given a set of t trial segments $X_t \in \mathbb{R}^{d\times N}$, where d is the number of channels and N represents number of samples, within-trial covariance matrices $\mathbf{\Sigma}_t = X_t X_t^T$ and within-class average covariance matrices $\mathbf{\Sigma}^c = \langle \mathbf{\Sigma}_t^c \rangle$ one can solve the following optimization problem to find the optimal filter:

$$\begin{aligned} &\arg\max_{\mathbf{w}} \mathbf{w}^T \mathbf{\Sigma}^{(\mathbf{c})} \mathbf{w} \\ &\text{such that } \mathbf{w}^T(\mathbf{\Sigma}^{(\mathbf{c_0})} + \mathbf{\Sigma}^{(\mathbf{c_1})})\mathbf{w} = 1 \end{aligned}$$

where $\mathbf{c}_0$ represents class 0 and $\mathbf{c}_1$ represents class 1. The term $\arg\max_{\mathbf{w}} \mathbf{w}^T \mathbf{\Sigma}^{(\mathbf{c})} \mathbf{w}$ gives the variance in the direction $\mathbf{w}$. Solving a generalized eigenvalue problem can give the

solution for the stated optimization problem. Given the within-class covariance matrices $\mathbf{\Sigma}^c$, one can find a simultaneous diagonalizer $\boldsymbol{V}$ of $\mathbf{\Sigma}^{(c_0)}$ and $\mathbf{\Sigma}^{(c_1)}$ with:

$$\begin{aligned} \mathbf{V}^T\mathbf{\Sigma}^{(\mathbf{c_0})}\mathbf{V} &= \mathbf{D}^{(c_0)} \\ \mathbf{V}^T\mathbf{\Sigma}^{(\mathbf{c_1})}\mathbf{V} &= \mathbf{D}^{(c_1)} \end{aligned} \tag{2.13}$$

This will result in the following generalized eigenvalue problem:

$$\mathbf{D}\Lambda\mathbf{V}^T(\mathbf{\Sigma}^{(\mathbf{c_0})} + \mathbf{\Sigma}^{(\mathbf{c_1})})\mathbf{V} = \mathbf{I} \tag{2.14}$$

where k smallest and largest eigenvalues in $\mathbf{D}$ will correspond to k leftmost or rightmost columns in $\mathbf{V}$, which will yield in the spatial filters that have smallest variance in class 0 while simultaneously having largest variance in class 1, and vice versa. By solving this problem, one can achieve maximum separability across two classes.

In our study, we have used MNE-Python [27] package to utilize common spatial patterns as a feature extraction algorithm. The patterns can also be projected onto a scalp with given electrodes and one such example can be seen in Fig. 7.

2.3.2 Classification between Stroke Patients with and without Spatial Neglect for Neglect Assessment

To develop a classification algorithm based on the recorded EEG that will distinguish between stroke patients with and without neglect, we utilize a deep learning methodology based on convolutional neural network (CNN) structures. Such deep learning structures have been used to develop classification and object recognition algorithms for various applications [40]. For example, they are used to analyze time-series data [26] for speech recognition [2], time-series classification [55] and stock price prediction [28]. Recently, there have been attempts to analyze EEG data using deep CNN structures [46] both in time [54] and frequency domains [30]. In this paper, we consider EEG data as a multi-channel time-series and develop a classifier to detect neglect. Our experimental results with stroke patients show that our method can detect neglect with high accuracy, specificity and sensitivity. More specifically, we developed a classification algorithm to distinguish between the preprocessed and

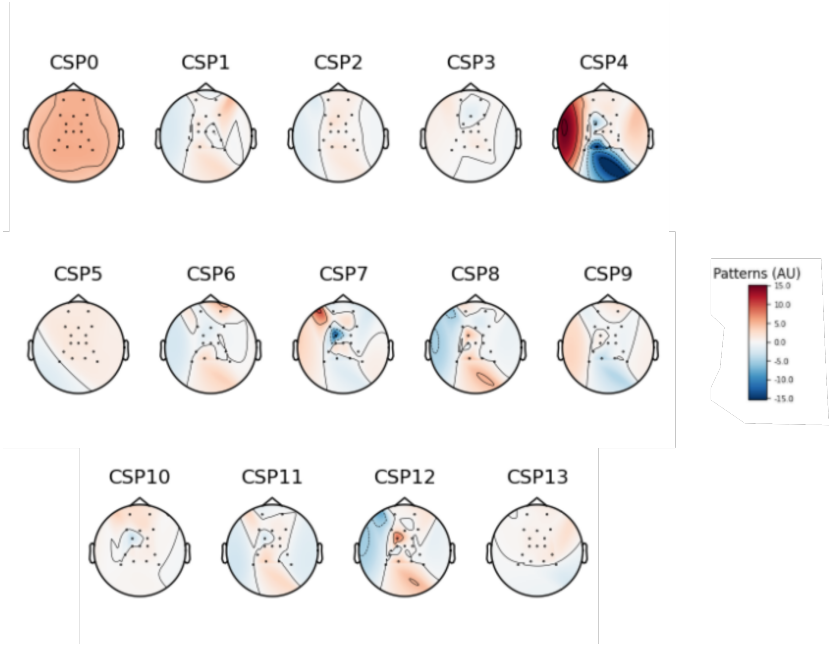

Figure 7: Spatial patterns of SN01.

segmented EEG data corresponding to the slow-response targets for stroke patients with and without neglect. To achieve this goal, we utilized EEGNet [39] to build this classifier. EEGNet includes a CNN model that can be applied to recorded multi-channel EEG. EEGNet is paradigm agnostic and can be trained with limited EEG data. As our results below demonstrate, we identified that the CNN structures in EEGNet are more robust to overfitting to training data and outliers in the recorded EEG with high generalization.

2.3.2.1 EEGNet - Neural Network-based Classifier

The classification approach/structure is depicted in Fig 8. In this classification method, a 2D convolutional layer (a temporal filter) with a size of $(30, 1)$ is followed by a batch normalization and a depthwise convolution [12] layer of size $(1, 16)$ (a spatial filter). Depthwise convolution is used to reduce the number of trainable parameters and most importantly, in EEG applications, such a filtering approach allows us to train spatial filters (based on electrode location) for each temporal filter output. A batch normalization [29] layer is then

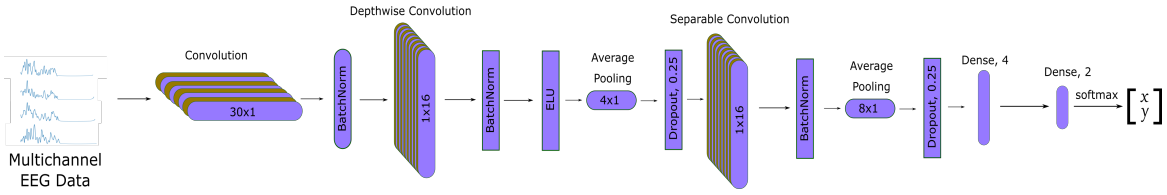

Figure 8: The structure of the classification framework for SN detection. (©2020 IEEE)

applied along the extracted spatiotemporal features. These features are then processed through an exponential linear unit [13] and an average pooling layer of size $(4, 1)$ to reduce computational complexity. After these layers, a dropout [48] with a rate of 0.25 is applied. Note that throughout this process in each convolutional layer, we regularize each filter with a maximum norm constraint of 1 on its weights and use L2 kernel regularization to further avoid overfitting [16].

The model continues with a separable convolution layer [12] with the same size as the depthwise layer, $(1, 16)$. Separable convolution layers are depthwise convolution layers followed by pointwise convolutions. Such an approach reduces the number of parameters while the pointwise convolution optimally combines the extracted spatiotemporal features. Before the final step an average pooling layer of size $(8, 1)$ is used for further dimension reduction.

The model concludes with the classification layer. Specifically, the output of the last average pooling layer is flattened to a vector, then fed to a fully connected layer with 4 units, followed by a final layer with 2 units to classify. To get classification probabilities, the model ends with softmax activation layer.

3.0 Results and Discussion

We have conducted three different analysis for two different cases: an across-participants analysis for spatial neglect detection across stroke participants, and across-participants analysis for slow response versus fast response analysis and participant-wise assessment.

3.1 Participants

As there are two different analyses, we have used two different participant sets.

3.1.1 Participants for Spatial Neglect Detection

11 stroke patients: 5 patients with SN and 6 patients without SN (WSN) participated in the experiments. Experimental procedures were approved by the Institutional Review Board (IRB) of the University of Pittsburgh (IRB number PRO15020115). Participants must score at least 8/10 on a visual acuity test to be eligible. Once the eligibility was confirmed, BIT was administered to determine the presence or absence of neglect. A diagnosis of neglect was established by either a total BIT score lower than the established cutoff (<129), or a score lower than the cutoff score on more than one subtest [52]. Patients with recent seizures were excluded from this study. Patient characteristics are detailed in Table 2. Note that SN04 is missing time since stroke information.

3.1.2 Participants for Across Participants Analysis for Slow- versus Fast-response Targets

A total of 10 stroke patients, 5 with spatial neglect (SN) and 5 without SN participated in the experiments. Five of those patients (4 with SN, 1 without SN) have participated in a previously conducted experiment [30, 49], which were approved by the Institutional Review Board (IRB) of the University of Pittsburgh (IRB number PRO15020115). The remaining

Table 1: Participant Characteristics for Computer-based BCI. (©2019 IEEE)

	Age	Sex	Stroke Hemisphere	Days Since Stroke	BIT Total	BIT subtests below cutoff (/6)
SN01	76	M	Right	115	44	6
SN02	51	M	Right	9	25	5
SN03	67	M	Right	3	127	5
SN04	72	F	Right	-	130	2
SN05	57	F	Left	7	134	2
WSN01	68	F	Right	17	139	1
WSN02	80	M	Left	21	140	0
WSN03	66	F	Left	10	142	1
WSN04	69	M	Left	5	143	0
WSN05	57	M	Left	8	145	0
WSN06	69	F	Bilateral	10	146	0

patients have been through the new experimental procedures which were approved by the IRB of the University of Pittsburgh (IRB number STUDY19060390). Patient characteristics are given in Table 2. Participants that scored below the overall cutoff score of 129 on the BIT, or have more than two subtests that are below the subtest cutoff scores are considered to have spatial neglect. Days since stroke indicate chronicity. To inform analyses, patients with identification numbers starting with 0 are from previously collected data, and those starting with 1 are collected using AREEN architecture.

3.2 Spatial Neglect Detection Across Stroke Participants

We present here the results for classification between recorded EEG responses corresponding to the slow-time responses for stroke patients with and without neglect to demonstrate the performance of the proposed approach for neglect detection. In our approach, the proposed CNN-based deep learning model was implemented using Tensorflow [1].Here the classification/ neglect detection results are obtained through 10-fold cross validation. For each training set, the model was trained from the start for 100 epochs and each network was trained with a mini-batch size of 16. We chose categorical cross-entropy as the loss function

Table 2: Participant Characteristics for AREEN Data.

ID	Age	Sex	Stroke Hemisphere	Days Since Stroke	BIT Total	BIT Subtests Below Cutoff
SN01	76	M	Right	115	44	6
SN02	51	M	Right	9	25	5
SN04	72	F	Right	-	130	2
SN05	57	F	Left	7	134	2
SN101	81	F	Right	701	107	3
WSN01	68	F	Right	17	139	1
WSN101	35	M	Left	2404	138	0
WSN102	57	F	Left	2466	145	0
WSN103	80	M	Right	823	142	0
WSN104	27	M	Left	483	146	0

and Adam [33] as the optimizer, with parameters $\alpha = 10^{-3}$, $\beta_1 = 0.9$ and $\beta_2 = 0.999$. We did not explicitly set any weight decays. The model had approximately 1400 trainable parameters and each optimization of epoch lasted for approximately 3 seconds on CPU. We observed for the training data that in average neglect detection accuracy, specificity, sensitivity, and F1 score are 90.65%, 90.32%, 87.13%, and 0.9223 respectively.

The results obtained from the test data are listed on Table 3. On this table, in each row average values demonstrate the results for each test data of the 10-fold cross validation. Even though the training set results are better than the test set results, we observe from Table 3 that overall accuracy, specificity and sensitivity were calculated on average to be 89.73%, 89.34%,and 86.97%, respectively, with an F1 score of 0.8934. Specificity is the accuracy of detecting the neglected targets while sensitivity is the accuracy of detecting non-neglected targets. These results demonstrate that the proposed approach generalizes to test data with high performance. Moreover, through an in depth analysis of our results, we observe that to detect neglect Cz, P1 and F3 as the most informative channels.

These results show that the neural network model is efficient in detecting existence of spatial neglect in acute stroke patients. As the model is trained over only potentially neglected targets from both of the participant categories, it successfully detects a pattern

Table 3: Summary of Performance Measures for Neglect Detection. (©2020 IEEE)

Cross Validation	**Accuracy**	**Specificity**	**Sensitivity**	**F1 Score**
Set 1	89.21%	88.43%	87.32%	0.8842
Set 2	88.41%	88.89%	87.26%	0.8889
Set 3	90.29%	90.62%	87.56%	0.9062
Set 4	88.49%	88.31%	86.48%	0.8831
Set 5	91.37%	90.51%	86.45%	0.9051
Set 6	88.40%	88.89%	87.38%	0.8889
Set 7	92.03%	91.31%	86.83%	0.9131
Set 8	89.50%	86.80%	87.21%	0.8680
Set 9	89.85%	90.28%	86.21%	0.9028
Set 10	90.22%	89.58%	86.60%	0.8958
Average	89.73%	89.34%	86.97%	0.8934

in ERP's. By definition, class 1 data is from stroke patients with spatial neglect. More specifically, high sensitivity means that the model is successful in detecting the existence of neglect. F1 score is the harmonic mean of precision and recall and it gives a better measure of the incorrectly classified labels compared to accuracy. High F1 score also means that even though there is an uneven class distribution in our database, it also shows that our model is generalizable.

3.3 Across-Participants Analysis for Slow vs. Fast Response Targets

Here, we present the results for classification between recorded EEG responses corresponding to the slow-response and fast-response targets for stroke patients with and without spatial neglect to show the performance of our proposed classifier for neglect detection. The results in Table 4 are obtained through 10-fold cross validation. For each training set, the model was trained from scratch.

The results obtained from the test data are shown in Table 4. On this table, average values in each row show the results for each test data of the 10-fold cross validation. Best

Table 4: Summary of Performance Measures for Slow vs Fast Response Analysis

Training Set	Accuracy	Specificity	Sensitivity	Test Accuracy	Test Specificity	Test Sensitivity
Training Set 1	87.7%	92.1%	77.4%	84.5%	87.3%	72.7%
Training Set 2	88.3%	93.8%	82.4%	82.1%	86.4%	78.7%
Training Set 3	82.7%	88.1%	83.9%	79.2%	84.3%	81.2%
Training Set 4	88.4%	96.6%	76.3%	81.3%	84.6%	81.8%
Training Set 5	77.1%	83.7%	83.4%	83.4%	87.2%	81.8%
Training Set 6	82.7%	85.4%	77.4%	81.5%	84.6%	79.2%
Training Set 7	80.4%	82.2%	84.9%	81.3%	86.6%	81.8%
Training Set 8	89.3%	94.3%	87.6%	**87.9%**	**92.2%**	**87.6%**
Training Set 9	82.4%	92.8%	79.4%	81.9%	82.4%	82.2%
Training Set 10	84.6%	95.2%	78.9%	84.4%	81.2%	80.3%
Average	84.4 ±3.8%	90.4 ±4.9%	81.1 ±3.6%	82.7 ±2.3%	85.6 ±2.9%	80.7 ±3.5%

metrics over all sets are also denoted. Even though training results are superior compared to demonstrated results, one can observe that the overall accuracy, specificity and sensitivity show that the proposed method generalizes to test data with high performance as well.

Here, one can see that there is a continuity in training and test set metrics. In the last row, average metrics with their respective standard deviations are given. Accuracy and specificity values are high and sensitivity values are relatively low compared to those two metrics. It concludes that even though the model is highly accurate in predicting existence of neglect it works better for detecting absence of it.

LDA is a traditional, more basic classifier compared to neural networks. In addition to these results, we have utilized the same EEGNet network for detecting potentially neglected targets. We have used the same parameters in this analysis, as given in Section 2.2.2. Here, we also used only the first 14 channels as we have used data from both of the paradigms presented. Also, we utilized filtered EEG data in time-domain as our dataset without using any feature extraction methods. The model works with 88.2% accuracy, 94.7% specificity and 64.3% sensitivity. By definition, 'class 1' is slow-response targets, also known as potentially neglected targets. By comparing these results to those that are in 4 one can see that even though accuracy has become higher with this deep learning model, sensitivity is decreased

drastically. Specifically, the deep learning model is working poorer compared to LDA in terms of detecting potentially neglected targets, and higher accuracy can be explained with two problems in our dataset: class imbalance and relatively small dataset.

3.3.1 Participant-wise Estimation

After getting these cross-validation set results, we have also conducted a participant-wise estimation analysis. In this analysis, we have set a specific participant's data for testing and left the remainder as training data. Then, half of that participant's data is taken and put into the training dataset as EEG is a very person-specific data [41]. The aim in this analysis is to see whether the model is generalizable enough to assess a single participant's EEG data. This is also an approach for domain adaptation: collecting EEG data from stroke patients is challenging and model generalization for our dataset requires substantial amount of data. We have reported the accuracies associated with each participant which can be seen in Table 5.

Table 5: Participant-wise Analysis

Participant	**LOO Accuracy**	**LHO Accuracy**
SN01	45.6%	65.4%
SN02	32.2%	75.1%
SN04	56.7%	71.6%
SN05	53.6%	74.0%
SN101	72.9%	84.5%
WSN01	86.4%	87.8%
WSN101	73.6%	79.7%
WSN102	82.2%	87.4%
WSN103	54.9%	79.3%
WSN104	41.6%	90.0%

Actual number of slow-response or fast-response targets differ by huge margins from participant to participant, but one can see that the accuracies are high for each participant. Even though in Table 5 has less metrics compared to other analysis tables, this research is equally important. This project's scope is creating a way to develop a setup for healthcare providers for rehabilitation of acute stroke patients with spatial neglect. This makes way for building up on the model for rehabilitating stroke patients.

4.0 Conclusion and Future Work

In this paper, we have developed and tested an EEG-based BCI for spatial neglect detection. For neglect detection and EEG analysis, we utilized a CNN-based deep learning model to identify EEG features not only in time domain, but also in the spatial domain to improve the detection of neglect across stroke patients with and without neglect. We also showed that our approach can detect neglect with high accuracy, specificity and sensitivity generalizing from training to test data. We have also presented our AREEN system that incorporates an augmented reality (AR) headset into a BCI framework, and developed and tested an EEG-based BCI for spatial neglect detection. For the EEG analysis, we utilized common spatial patterns and linear discriminant analysis to identify EEG features. We have also shown that our method is highly accurate and generalizable in detecting neglect with high accuracy, specificity and sensitivity. By conducting a participant-wise analysis, we show that our BCI setup is working with high accuracy even without seeing that specific participant's entire data. Future research will use the proposed AREEN system to be implemented in rehabilitation of patients with SN. Specifically, a realtime feedback system for patients with SN will be developed for rehabilitation; visual and auditory feedback will be given to the participant by processing EEG data in a realtime sense.

Appendix Neural Network Concepts and Layers in EEGNet

A.1 Dataset

A generic dataset consists of input-output pairs $(\mathbf{x}, \mathbf{y})$ where $\mathbf{x}$ are input and $\mathbf{y}$ are desired outputs. In this study, $\mathbf{x}$ are either common spatial pattern data or filtered time-series EEG data, and $\mathbf{y}$ are the labels: either defining if the corresponding data is from a participant with or without neglect, or if the corresponding data is a slow response or a fast response target.

A.2 Feedforward Neural Network

Feedforward neural networks are artifical neural networks where connections between the nodes do not form a cycle. There are n layers in a feedforward neural network: an input layer, an output layer and $n-2$ hidden layers.

A.3 Backpropagation

Backpropagation of errors, or generalized delta learning rule, is the algorithm that is used for training feedforward neural network models [36]. To fit a neural network, backpropagation computes the gradient of the loss function with respect to the weights of the network. To efficiently compute this, backpropagation computes the loss function for a single input-output sample and this makes way to use gradient methods for training multilayer networks. This is possible because backpropagation does the calculation by computing the gradient of the loss function with respect to each weight by the chain rule: computing the gradient of one layer at a time and iterating it backward from the last layer to avoid reduntant calculations of middle terms in the chain rule, hence the name backpropagation. Backpropagation of

errors for a network with m number of hidden layers where $m > 0$ changes the weights in a direction of the negative derivative:

$$W^{NEW} = W - \eta \frac{dE}{dW} \tag{.1}$$

where η is the learning rate. The error for given l-th learning example and error of the i-th output neuron are defined as:

$$E(l) = \frac{1}{2} \sum_{i=1}^{N_Y} e_i^2(l) \tag{.2}$$

$$e_i(l) = d(l) - Y_i(l) \tag{.3}$$

We now use partial derivatives with respect to weights $W_{ji}^{(m+1)}$ with chain rule:

$$\frac{\partial E(l)}{\partial W_{ji}^{(m+1)}} = \frac{\partial E(l)}{\partial e_i(l)} \frac{\partial e_i(l)}{\partial Y_i(l)} \frac{\partial Y_i(l)}{\partial A_i(l)} \frac{\partial A_i(l)}{\partial W_{ji}^{(m+1)}} \tag{.4}$$

where A_i are the activation levels of output neurons. The particular partial derivatives have the results of $e_i(l)$, -1, $f'(A_i(l))$ and $H_{mj}(l)$ where f' is a derivative of the output function and H_{mj} is the output of m-th hidden layer. Thus, the rule to update the weights $W^{(m+1)}$ of output neurons is:

$$\begin{aligned} W_{ji}^{NEW(m+1)} &= W_{ji}^{(m+1)} - \eta \frac{\partial E(l)}{\partial W_{ji}^{(m+1)}} \\ &= W_{ji}^{(m+1)} + \eta e_i(l) f'(A_i(l)) H_{mj}(l) \end{aligned} \tag{.5}$$

and the general rule for updating hidden layers is:

$$W_{ji}^{NEW(k)} = W_{ji}^{(k)} - \eta \frac{\partial E(l)}{\partial A_{ki}(l)} H_{k-1,j}(l) \tag{.6}$$

For the first hidden layer ($k = 1$), $H_{k-1,j}(l)$ becomes $X_j(l)$ as the layer before the first hidden layer is the input layer.

A.4 Loss Function

A loss function is simply a measure of error between a ground-truth value and its prediction by a model. Regression losses such as mean squared error or Huber loss, hinge losses and probabilistic losses such as Poisson loss or cross-entropy loss are popular for neural network models. In our modality, we have used cross-entropy loss for binary classification.

Categorical cross-entropy loss calculates

$$Loss = -\sum_{i=1}^{n} y_i \log \hat{y}_i \tag{.7}$$

where n is the output size, $\hat{y}_i$ is the i-th scalar value in the model output, y_i is the corresponding ground-truth. y_i is the probability for event i to occur; thus, $\sum_i y_i = 1$. This loss measures how distinguishable two discrete probability distributions are from each other.

A.5 Layers in EEGNet

A.5.1 Convolutional Layer

Convolutional layers are in most basic sense, layers that convolve the input with the kernel to provide an output.

A.5.2 Rectifying Linear Unit (ReLU)

Rectifying linear units employ a rectifier, which is an activation function defined as the positive part of its argument. The main purpose of activation functions is that they introduce non-linearity into the network.

$$f(x) = x^+ = max(0, x) \tag{.8}$$

They are the most popular non-linear activators that are used in the neural network models for two main reasons. First, they make the model computationally easier to run: they are idempotent, the gradient calculation is rather simple as it is constant, which also counters

the vanishing gradient problem. Second reason is convergence, as it is shown that ReLU activators show better convergence performance than sigmoid function [38].

A.5.3 Flatten Layer

This layer flattens the n-dimensional input layer into a vector.

A.5.4 Softmax Function

Softmax function is often used as the last activation function of a neural network model to normalize the total output of the model to a probability distribution over predicted output classes. Softmax function is defined as:

$$\sigma(z)_i = \frac{e^{z_i}}{\sum_{j=1}^{K} e^{z_i}} \; for \; i = 1, ..., K \; and \; \mathbf{z} = (z_1, ..., z_K) \in \mathbb{R}^K \tag{.9}$$

where $\mathbf{z}$ is the input vector of K elements and $\sigma(z)$ is the output vector where $\sigma : \mathbb{R}^K \rightarrow [0, 1]^K$. Basically, exponential function is applied to each element of $\mathbf{z}$ and they are normalized by dividing by the sum of all of the exponentials so that the sum of the components of $\sigma(\mathbf{z})$ is 1.

A.5.5 Dropout Layer

Dropout layers set hidden outputs of the layers to zero with a given probability [48]. These layers are used to inhibit overfitting.

A.5.6 Batch Normalization Layer

Batch normalization layer normalizes the input layer by recentering and rescaling to make neural network models to be more stable and run faster [29].

$$\mu_b = \frac{1}{m}\sum_{i=1}^{m} x_i \tag{.10}$$

$$\sigma_b^2 = \frac{1}{m}\sum_{i=1}^{m}(x_i - \mu_b)^2 \tag{.11}$$

$$\hat{x}_i = \frac{x_i - \mu_b}{\sqrt{\sigma_b^2 + \epsilon}} \tag{.12}$$

$$y_i = \gamma\hat{x}_i + \beta \equiv BN_{\gamma,\beta}(x_i) \tag{.13}$$

where μ_b is the mini-batch mean, σ_b^2 is the mini-batch variance, $\hat{x}_i$ is normalized x_i and at the end we have the scaled and shifted version of x_i. γ and β are scale and offset parameters respectively and they are actively learned in the training process.

Bibliography

[1] Martín Abadi, Paul Barham, Jianmin Chen, Zhifeng Chen, Andy Davis, Jeffrey Dean, Matthieu Devin, Sanjay Ghemawat, Geoffrey Irving, Michael Isard, et al. Tensorflow: A system for large-scale machine learning. In *12th {USENIX} Symposium on Operating Systems Design and Implementation ({OSDI} 16)*, pages 265–283, 2016.

[2] O. Abdel-Hamid, A. Mohamed, H. Jiang, L. Deng, G. Penn, and D. Yu. Convolutional Neural Networks for Speech Recognition. *IEEE/ACM Transactions on Audio, Speech, and Language Processing*, 22(10):1533–1545, Oct 2014.

[3] Murat Akcakaya, Betts Peters, Mohammad Moghadamfalahi, Aimee R. Mooney, Umut Orhan, Barry Oken, Deniz Erdogmus, and Melanie Fried-Oken. Noninvasive brain-computer interfaces for augmentative and alternative communication. *IEEE reviews in biomedical engineering*, 7:31–49, 2014.

[4] B Anderson, M Mennemeier, and A Chatterjee. Variability not ability: another basis for performance decrements in neglect. *Neuropsychologia*, 38(6):785–796, 2000.

[5] P Appelros. Prediction of Length of Stay for Stroke Patients. *Acta Neurologica Scandinavica*, 116(1):15–19, 2007.

[6] Philippe Azouvi, Sylvie Olivier, Godeleine de Montety, Christiane Samuel, Anne Louis-Dreyfus, and Luigi Tesio. Behavioral assessment of unilateral neglect: study of the psychometric properties of the catherine bergego scale. *Archives of physical medicine and rehabilitation*, 84:51–7, Jan 2003.

[7] Antonello Baldassarre, Lenny Ramsey, Carl Hacker, Alicia Callejas, Serguei Astafiev, N.V. Metcalf, Kristi Zinn, Jennifer Rengachary, Abraham Snyder, Alex Carter, Gordon Shulman, and Maurizio Corbetta. Large-Scale Changes in Network Interactions as a Physiological Signature of Spatial Neglect. *Brain*, 137:3267–3283, Nov 2014.

[8] Daniela Balslev and Bartholomäus Odoj. Distorted gaze direction input to attentional priority map in spatial neglect. *Neuropsychologia*, 131:119–128, Aug 2019.

[9] Elisabeth Becker and Hans-Otto Karnath. Incidence of Visual Extinction After Left Versus Right Hemisphere Stroke. *Stroke*, 38:3172–3174, Jan 2008.

[10] Laurel J Buxbaum, MK Ferraro, T Veramonti, A Farne, JMDP Whyte, E Ladavas, F Frassinetti, and HB Coslett. Hemispatial Neglect: Subtypes, Neuroanatomy, and Disability. *Neurology*, 62(5):749–756, 2004.

[11] Peii Chen, Kimberly Hreha, Yekyung Kong, and AM Barrett. Impact of Spatial Neglect on Stroke Rehabilitation: Evidence from the Setting of an Inpatient Rehabilitation Facility. *Archives of Physical Medicine and Rehabilitation*, 96(8):1458–1466, 2015.

[12] François Chollet. Xception: Deep Learning with Depthwise Separable Convolutions. *CoRR*, abs/1610.02357, 2016.

[13] Djork-Arné Clevert, Thomas Unterthiner, and Sepp Hochreiter. Fast and Accurate Deep Network Learning by Exponential Linear Units (ELUs). *CoRR*, abs/1511.07289, 2015.

[14] Giorgia Committeri, Sabrina Pitzalis, Gaspare Galati, Fabiana Patria, Gina Pelle, Umberto Sabatini, Alessandro Castriota Scanderbeg, Laura Piccardi, Cecilia Guariglia, and Luigi Pizzamiglio. Neural Bases of Personal and Extrapersonal Neglect in Humans. *Brain*, 130:431–441, Mar 2007.

[15] Maurizio Corbetta, Michelle J. Kincade, Chris Lewis, Abraham Z. Snyder, and Ayelet Sapir. Neural basis and recovery of spatial attention deficits in spatial neglect. *Nature neuroscience*, 8:1603–10, Nov 2005.

[16] Corinna Cortes, Mehryar Mohri, and Afshin Rostamizadeh. L2 Regularization for Learning Kernels. *CoRR*, abs/1205.2653, 2012.

[17] Leon Y. Deouell, Yaron Sacher, and Nachum Soroker. Assessment of Spatial Attention After Brain Damage with a Dynamic Reaction Time Test. *Journal of the International Neuropsychological Society*, 11(6):697–707, 2005.

[18] Francesco Di Russo, Teresa Aprile, Grazia Spitoni, and Donatella Spinelli. Impaired visual processing of contralesional stimuli in neglect patients: a visual-evoked potential study. *Brain*, 131(3):842–854, 2007.

[19] Francesco Di Russo, Teresa Aprile, Grazia Spitoni, and Donatella Spinelli. Impaired visual processing of contralesional stimuli in neglect patients: a visual-evoked potential study. *Brain : a journal of neurology*, 131:842–54, Mar 2008.

[20] Frédéric Faugeras and Lionel Naccache. Dissociating temporal attention from spatial attention and motor response preparation: A high-density eeg study. *NeuroImage*, 124:947–957, 2016-01.

[21] R. A. FISHER. The use of multiple measurements in taxonomic problems. *Annals of Eugenics*, 7(2):179–188, 1936.

[22] Robert S Fisher, Graham Harding, Giuseppe Erba, Gregory L Barkley, and Arnold Wilkins. Photic-and pattern-induced seizures: a review for the epilepsy foundation of america working group. *Epilepsia*, 46(9):1426–1441, 2005.

[23] Robert S Fisher, Graham Harding, Giuseppe Erba, Gregory L Barkley, and Arnold Wilkins. Photic-and pattern-induced seizures: a review for the epilepsy foundation of america working group. *Epilepsia*, 46(9):1426–1441, 2005.

[24] Ronald A Fisher. The use of multiple measurements in taxonomic problems. *Annals of eugenics*, 7(2):179–188, 1936.

[25] Julius Fridriksson, Chris Rorden, Paul S. Morgan, K. Leigh Morrow, and Gordon C. Baylis. Measuring the hemodynamic response in chronic hypoperfusion. *Neurocase*, 12(3):146–150, 2006. PMID: 16801150.

[26] John Cristian Borges Gamboa. Deep Learning for Time-Series Analysis. *CoRR*, abs/1701.01887, 2017.

[27] Alexandre Gramfort, Martin Luessi, Eric Larson, Denis Engemann, Daniel Strohmeier, Christian Brodbeck, Roman Goj, Mainak Jas, Teon Brooks, Lauri Parkkonen, and Matti Hämäläinen. Meg and eeg data analysis with mne-python. *Frontiers in Neuroscience*, 7:267, 2013.

[28] M. Hiransha, E.A. Gopalakrishnan, Vijay Krishna Menon, and K.P. Soman. NSE Stock Market Prediction Using Deep-Learning Models. *Procedia Computer Science*, 132:1351–1362, 2018.

[29] Sergey Ioffe and Christian Szegedy. Batch Normalization: Accelerating Deep Network Training by Reducing Internal Covariate Shift. *CoRR*, abs/1502.03167, 2015.

[30] Aya Khalaf, Jessica Kersey, Safaa Eldeeb, Gazihan Alankus, Emily Grattan, Laura Waterstram, Elizabeth Skidmore, and Murat Akcakaya. EEG-based Neglect Assessment: A Feasibility Study. *Journal of Neuroscience Methods*, 303:169–177, June 2018.

[31] J. Michelle Kincade, Richard A. Abrams, Serguei V. Astafiev, Gordon L. Shulman, and Maurizio Corbetta. An event-related functional magnetic resonance imaging study of voluntary and stimulus-driven orienting of attention. *Journal of Neuroscience*, 25(18):4593–4604, 2005.

[32] Christine E. King, Po T. Wang, Colin M. McCrimmon, Cathy C. Y. Chou, An H. Do, and Zoran Nenadic. Brain-computer interface driven functional electrical stimulation system for overground walking in spinal cord injury participant. *Annual International Conference of the IEEE Engineering in Medicine and Biology Society. IEEE Engineering in Medicine and Biology Society. Annual International Conference*, 2014:1238–42, 2014.

[33] Diederik Kingma and Jimmy Ba. Adam: A Method for Stochastic Optimization. *International Conference on Learning Representations*, December 2014.

[34] Mario Kleiner, D.H. Brainard, Denis Pelli, A. Ingling, R. Murray, and C. Broussard. What's New in Psychtoolbox-3. *Perception*, 36:1–16, Jan 2007.

[35] Zoltan J. Koles, Michael S. Lazar, and Steven Z. Zhou. Spatial patterns underlying population differences in the background eeg. *Brain Topography*, 2(4):275–284, 1990.

[36] Igor Kononenko and Matjaz Kukar. *Machine Learning and Data Mining: Introduction to Principles and Algorithms*. Horwood Publishing Limited, 2007.

[37] Aziz Koçanaoğulları, Yeganeh M. Marghi, Murat Akçakaya, and Deniz Erdoğmuş. An active recursive state estimation framework for brain-interfaced typing systems. *Brain-Computer Interfaces*, 6(4):149–161, 2019.

[38] Alex Krizhevsky, Ilya Sutskever, and Geoffrey E Hinton. Imagenet classification with deep convolutional neural networks. In F. Pereira, C. J. C. Burges, L. Bottou, and K. Q. Weinberger, editors, *Advances in Neural Information Processing Systems*, volume 25. Curran Associates, Inc., 2012.

[39] Vernon J. Lawhern, Amelia J. Solon, Nicholas R. Waytowich, Stephen M. Gordon, Chou P. Hung, and Brent J. Lance. EEGNet: A Compact Convolutional Network for EEG-based Brain-Computer Interfaces. *CoRR*, abs/1611.08024, 2016.

[40] Yann LeCun, Yoshua Bengio, and Geoffrey Hinton. Deep learning. *Nature*, 521:436–444, May 2015.

[41] S. Marcel and J. D. R. Millan. Person authentication using brainwaves (eeg) and maximum a posteriori model adaptation. *IEEE Transactions on Pattern Analysis and Machine Intelligence*, 29(4):743–752, 2007.

[42] N. Otsu. A Threshold Selection Method from Gray-Level Histograms. *IEEE Transactions on Systems, Man, and Cybernetics*, 9(1):62–66, Jan 1979.

[43] G. Pfurtscheller, C. Guger, G. Müller, G. Krausz, and C. Neuper. Brain oscillations control hand orthosis in a tetraplegic. *Neuroscience letters*, 292:211–4, 2000.

[44] Prudence Plummer, Meg E Morris, and Judith Dunai. Assessment of Unilateral Neglect. *Physical Therapy*, 83(8):732–740, 08 2003.

[45] H. Ramoser, J. Muller-Gerking, and G. Pfurtscheller. Optimal spatial filtering of single trial eeg during imagined hand movement. *IEEE Transactions on Rehabilitation Engineering*, 8(4):441–446, 2000.

[46] Yannick Roy, Hubert J. Banville, Isabela Albuquerque, Alexandre Gramfort, Tiago H. Falk, and Jocelyn Faubert. Deep Learning-based Electroencephalography Analysis: A Systematic Review. *CoRR*, abs/1901.05498, 2019.

[47] Keiko Seki and Sumio Ishiai. Diverse patterns of performance in copying and severity of unilateral spatial neglect. *Journal of Neurology*, 243(1):1–8, Jan 1996.

[48] Nitish Srivastava, Geoffrey Hinton, Alex Krizhevsky, Ilya Sutskever, and Ruslan Salakhutdinov. Dropout: A Simple Way to Prevent Neural Networks from Overfitting. *Journal of Machine Learning Research*, 15:1929–1958, 2014.

[49] Deniz Kocanaogullari ©[2020] IEEE. Reprinted, Jennifer Mak, Jessica Kersey, Aya Khalaf, Sarah Ostadabbas, George Wittenberg, Elizabeth Skidmore, and Murat Akcakaya. Eeg-based neglect detection for stroke patients. In *2020 42nd Annual International Conference of the IEEE Engineering in Medicine Biology Society (EMBC)*, pages 264–267, 2020.

[50] M. Thimm, G. R. Fink, J. Küst, H. Karbe, and W. Sturm. Impact of alertness training on spatial neglect: a behavioural and fmri study. *Neuropsychologia*, 44:1230–46, 2006.

[51] M.E. Van Kessel, I.J.W. Van Nes, W.H. Brouwer, A.C.H. Geurts, and L Fasotti. Visuospatial asymmetry and non-spatial attention in subacute stroke patients with and without neglect. *Cortex*, 46(5):602 – 612, May 2010.

[52] B Wilson, J Cockburn, and P Halligan. Development of a Behavioral Test of Visuospatial Neglect. *Archives of Physical Medicine and Rehabilitation*, 68(2):98—102, February 1987.

[53] Jonathan R. Wolpaw and Dennis J. McFarland. Control of a two-dimensional movement signal by a noninvasive brain-computer interface in humans. *Proceedings of the National Academy of Sciences of the United States of America*, 101:17849–54, Dec 2004.

[54] Chai Tong Yuen, Woo San San, Tan Ching Seong, and Mohamed Rizon. Classification of human emotions from eeg signals using statistical features and neural network. *International Journal of Integrated Engineering*, 1(3), 2009.

[55] Yi Zheng, Qi Liu, Enhong Chen, Yong Ge, and J Leon Zhao. Time series classification using multi-channels deep convolutional neural networks. In *International Conference on Web-Age Information Management*, pages 298–310. Springer, 2014.